

Article

Exploring Radial Kernel on the Novel Forced SEYNHRV-S Model to Capture the Second Wave of COVID-19 Spread and the Variable Transmission Rate

Fehaid Salem Alshammari ^{1,*}  and Ezgi Akyildiz Tezcan ²

¹ Department of Mathematics and Statistics, Faculty of Science, Imam Mohammad Ibn Saud Islamic University, Riyadh 11432, Saudi Arabia

² Department of Physical Medicine and Rehabilitation, Cumra State Hospital, 42500 Cumra, Konya, Turkey; fakyildiz@imamu.edu.sa

* Correspondence: falshammari@imamu.edu.sa

Abstract: The transmission rate of COVID-19 varies over time. There are many reasons underlying this mechanism, such as seasonal changes, lockdowns, social distancing, and wearing face masks. Hence, it is very difficult to directly measure the transmission rate. The main task of the present paper was to identify the variable transmission rate (β_1) for a SIR-like model. For this, we first propose a new compartmental forced SEYNHRV-S differential model. We then drive the nonlinear differential equation and present the finite difference technique to obtain the time-dependent transmission rate directly from COVID-19 data. Following this, we show that the transmission rate can be represented as a linear combination of radial kernels, where several forms of radial kernels are explored. The proposed model is flexible and general, so it can be adapted to monitor various epidemic scenarios in various countries. Hence, the model may be of interest for policymakers as a tool to evaluate different possible future scenarios. Numerical simulations are presented to validate the prediction of our SEYNHRV and forced SEYNHRV-S models, where the data from confirmed COVID-19 cases reported by the Ministry of Health in Saudi Arabia were used. These confirmed cases show the second wave of the infected population in Saudi Arabia. By using the COVID-19 data, we show that our model (forced SEYNHRV-S) is able to predict the second wave of infection in the population in Saudi Arabia. It is well known that COVID-19 epidemic data cannot be accurately represented by any compartmental approach with constant parameters, and this is also true for our SEYNHRV model.

Keywords: contagion dynamics; time dependent transmission rate; COVID-19; forced SEYNHRV-S model; radial kernel; finite difference method

MSC: 34A08; 37N30



Citation: Alshammari, F.S.; Tezcan, E.A. Exploring Radial Kernel on the Novel Forced SEYNHRV-S Model to Capture the Second Wave of COVID-19 Spread and the Variable Transmission Rate. *Mathematics* **2022**, *10*, 1501. <https://doi.org/10.3390/math10091501>

Academic Editors: James P. Braselton, Martha L. Abell and Sophia Jang

Received: 20 March 2022

Accepted: 29 April 2022

Published: 1 May 2022

Publisher's Note: MDPI stays neutral with regard to jurisdictional claims in published maps and institutional affiliations.



Copyright: © 2022 by the authors. Licensee MDPI, Basel, Switzerland. This article is an open access article distributed under the terms and conditions of the Creative Commons Attribution (CC BY) license (<https://creativecommons.org/licenses/by/4.0/>).

1. Introduction

Throughout history, infectious diseases have impacted humanity, such as the flu, smallpox, polio, plagues, AIDS, SARS, and MARS. Now, coronavirus disease 2019, which is known as COVID-19, has been affecting humans since 2019. This is a serious pandemic and is currently affecting the whole world. As of 6 September 2021, over 220 million people worldwide have been diagnosed with COVID-19, and this number is increasing daily. COVID-19 is transmitted in droplets from infected people through coughing or sneezing or simply breathing them out [1].

The COVID-19 pandemic has created problems in public health systems and has led to an economic slowdown of the economy around the world. The pandemic has disrupted lives and has pushed hospital systems to their capacity. Governments have put in place several preventive measures to control the transmission of the disease, including internal

and external travel restrictions, school closures, mandated mask wearing, and partial or complete lockdowns.

It is well known that the essential mathematical tools for analyzing the development of epidemics are compartmental models. The predictions from these models can be used by governments and policymakers to take adequate measures to prevent or control the spread of a disease and to allocate economic resources. These models divide populations into different compartments, and people may move between these compartments. Scientists have studied these models extensively, and a significant number of papers have been published on this subject in the short interval from the beginning of 2020 [2].

The first SIR (Susceptible (S), Infected (I), and Recovered (R)) model was originally proposed in 1927 by Kermack and McKendrick [3], and since then, several generalizations have been considered by several authors. For example, Ivorra et al. [4] developed a θ -SEIHRD model, and they studied the particular case of China, obtaining good agreement between the reported data and the prediction of their model. This group recently added more compartments to their original model, called $\theta - ij$ -SVEIHQRD, and used COVID-19 data from Italy. They observed that vaccination alone might not be enough to avoid a new wave of infection but may reduce the number of infections. More compartments have now been added, making the models far more complex (see, for example, [5–8], to mention only a few of the most recent models).

This article considered a flexible extension of the SEYNHR model, which incorporates the temporal dynamics connected to the transmission rate parameter, which is one of the most critical indicators for epidemiologists. This article also considered the effects of vaccination on the epidemic spread. To do this, we extended the model by adding a vaccinated people compartment, thus obtaining the SEYNHRV-S scheme. There are many vaccine-related papers in the COVID-19 literature, in which several hypothetical scenarios have been analyzed based on different prioritization policies, and we mentioned one of them above. Other studies have also focused on combining vaccination with nonpharmaceutical interventions [8,9]. It is also well known that the vaccination of more than 60% of the population is enough for herd immunity. Mancuso et al. [10] used the compartmental model to show that future waves of COVID-19 can be prevented in the U.S. if one of the two vaccines (Pfizer or Moderna) offer a moderate level of cross-protection against the variant (at least 67%). Moreover, Ngonghala et al. [11] considered a similar problem to that considered herein, but they considered each wave with different parameters; therefore, our study is more general. Another useful study, which is also similar to our model, was that undertaken by Asamoah et al. [12,13]. They provided cost-effective analysis, sensitivity assessment, and optimal economic evaluation of the model, but they assumed a constant transmission rate.

The transmission rate is the key parameter to understanding the spread of COVID-19; this is defined as the ratio of all possible contacts between susceptible and infected persons that effectively result in a new infection per unit of time. The extraction, estimation, or driving of the average transmission rate is a crucial challenge in the epidemiology of contagious diseases. In practice, there are different factors that impact the transmission rate: (i) the coefficient of susceptibility (wearing masks), (ii) virulence factors, (iii) the number of contacts per unit of time (government policies), etc. [14].

In this article, we introduced a new forced SEYNHRV-S model, summarized in Figure 1, including susceptible, exposed, symptomatic, asymptomatic, hospitalized, recovered, and vaccinated compartments. This model consists of a total of seven compartments and considers the impact of homestead isolation on the susceptible compartment. A similar model was originally introduced in [15], but deterministic cases, vaccinated populations, and the impact of homestead isolation on susceptible persons were not considered for a constant infection rate. Moreover, it is well known that compartmental approaches with constant parameters cannot represent COVID-19 data accurately. In order to overcome this problem, some authors have used variable parameters as a function of time, assuming that the infection rate is a function of the exponential or linear function of time, but we need

a more general mathematical representation. In this study, we proved that the infection rate can be represented as linear combinations of several forms of radial functions (kernels) in time, and we also provided numerical simulations to justify our results for the forced SEYNHRV-S model, where the data used are from COVID-19-confirmed cases reported by the Ministry of Health in Saudi Arabia (MOH). The model calibration was carefully tested by solving the constrained minimization problem using the weighted least square residuals between the measured epidemic data and the model predictions.

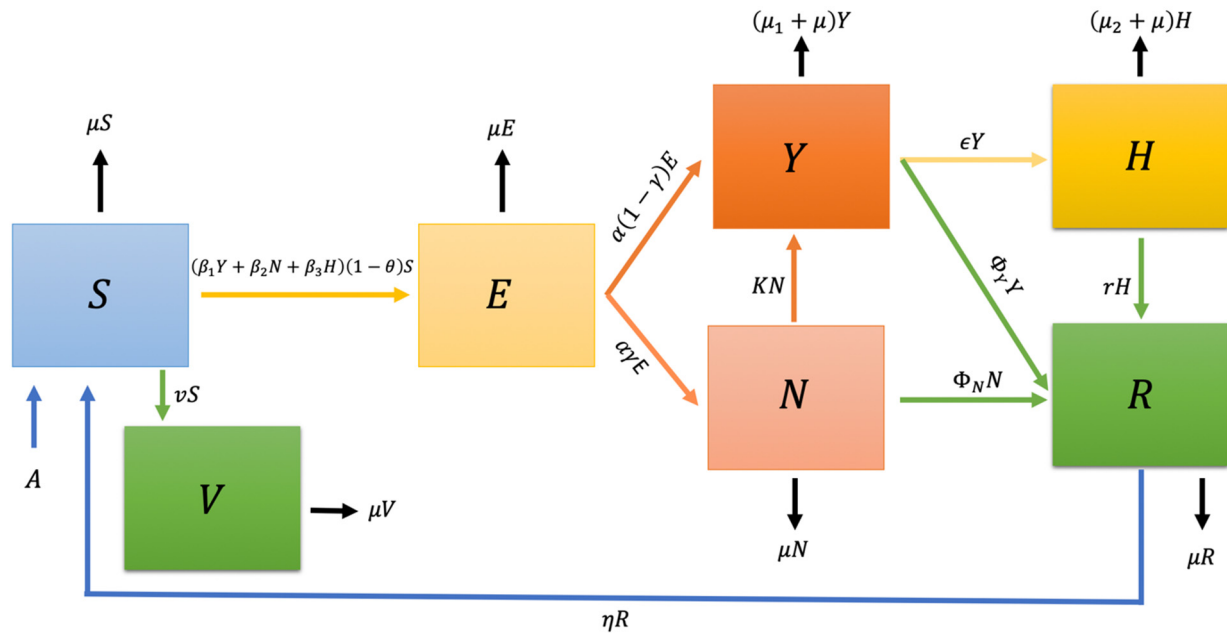


Figure 1. Schematic diagram of the compartmental epidemic model presented in Equation (1).

This paper is organized as follows: A detailed description of the model is presented in Section 2. In Section 3, we provide mathematical analysis and theory for radial functions. In Section 4, we derive nonlinear differential equations to obtain the time-dependent transmission rate function and provide a numerical solution. In Section 5, we provide a detailed numerical solution based on our new algorithm. Our original algorithm is as follows: We first found a numerical solution of the time-dependent transmission rate function; then, we proved that this can be represented by a linear combination of Gaussian radial functions, where we used the data from Saudi Arabia as an example, but our method can be applied to other countries with different COVID-19 data. We then solved the forced SEYNHRV-S model, which predicts the second wave, as confirmed by the data from Saudi Arabia. Some final remarks are presented in Section 5.

2. The Model

We considered the mathematical model with the presence of asymptomatic infections, as in [15], where the total population of humans denoted by Q is subdivided into the following groups: susceptible (S), exposed (E), symptomatic (Y), asymptomatic (N), hospitalized (H), and recovered (R), collectively termed SEYNHRV-S, which are represented in Figure 1 and related according to the following equations:

$$\left. \begin{aligned} \frac{dS}{dt} &= A - (\beta_1 Y + \beta_2 N + \beta_3 H)(1 - \theta)S - \mu S - \nu S + \eta R, \\ \frac{dE}{dt} &= (\beta_1 Y + \beta_2 N + \beta_3 H)(1 - \theta)S - (\alpha + \mu)E, \\ \frac{dY}{dt} &= \alpha(1 - \gamma)E - (\Phi_Y + \varepsilon + \mu_1 + \mu)Y + KN, \\ \frac{dN}{dt} &= \alpha\gamma E - (\Phi_N + K + \mu)N, \\ \frac{dH}{dt} &= \varepsilon Y - (r + \mu_2 + \mu)H, \\ \frac{dK}{dt} &= \Phi_Y Y + \Phi_N N + rH - \mu R - \eta R, \\ \frac{dV}{dt} &= \nu S - \mu V, \end{aligned} \right\} \quad (1)$$

with the initial conditions $(S(0), E(0), Y(0), N(0), H(0), R(0), V(0)) \geq 0$, where A represents the recruitment rate of the population; β_1, β_2 , and β_3 represent the transmission rates; $0 < \theta < 1$ represents the homestead isolation rate of susceptible persons; μ represents the natural death rate; $1/\alpha$ and γ represent the mean latent period and the probability of becoming asymptomatic after infection, respectively; the quantities $1/\Phi_Y$ and $1/\Phi_N$ represent the mean symptomatic and mean asymptomatic infectious periods, respectively; μ_1 and μ_2 represent the death rate of symptomatic and hospitalized patients, respectively; ε is the rate at which symptomatic patients become hospitalized; K is the rate at which asymptomatic persons become symptomatic; and r represents the rate of recovered hospitalized patients. In this model, η is the rate of the recovered population losing their immunity against the virus and becoming susceptible again. It can also be viewed as a factor that denotes the emergence of a mutated (and possibly more aggressive) variation of the virus, against which, recovered individuals have no immunity or their immunity is not good enough to protect them from the newly mutated virus. Meanwhile, the parameter ν represents the vaccination rate. Note that the total population $(Q(t))$ in Equation (1) is given by $S(t) + E(t) + Y(t) + N(t) + H(t) + R(t) + V(t) = Q(t)$ for $t \geq 0$. We also note that θ is set to zero throughout this study, unless stated otherwise.

3. Mathematical Analysis

In this section, we discuss the non-negativity of the solution.

Theorem 1. For the given initial conditions $(S(0), E(0), Y(0), N(0), H(0), R(0), V(0)) > 0$. The solution of the system in the SEYNHRV model (1) is non-negative for all $t > 0$.

Proof. We proofed this theorem by using contradiction principles. If time $\tau > 0$ does not exist, at least one of the unknown functions $S(\tau), E(\tau), Y(\tau), N(\tau), H(\tau), R(\tau)$, and $V(\tau)$ are nonpositive. Now, to use the continuity of the solution, t_0 must exist, such that at least one of the unknown functions $S(t_0), E(t_0), Y(t_0), N(t_0), H(t_0), R(t_0)$, and $V(t_0)$ are equal to 0. Without losing the generality, we may assume that t_0 is the minimal time for this property.

- (i) If $S(t_0) = 0$, then the other unknown functions are non-negative at t_0 . Hence, we obtained the following from the first differential equation in Equation (1):

$$\left. \frac{dS}{dt} \right|_{t=t_0} = A + \psi R > 0, \quad (2)$$

which tells us that we have $\varepsilon > 0$, such that $S(t)$ is strictly monotone, increasing on $(t_0 - \varepsilon, t_0 + \varepsilon)$.

Now, consider $t_2 \in (t_0 - \varepsilon, t_0)$. Then, $S(t_2) < S(t_0) = 0$, on the other hand, since $S(0) > 0$, there exists $t_3 \in (0, t_2)$ such that $S(t_3) = 0$ by Bolzano's theorem, which contradicts the assumption of t_0 . Hence, $S(t_0) > 0$.

- (ii) If $S(t_0) > 0$ and $E(t_0) = 0$, then the rest of the state variables are non-negative at t_0 ; Then, we have:

$$\left. \frac{dE}{dt} \right|_{t=t_0} = (\beta_1 Y(t_0) + \beta_2 N(t_0) + \beta_3 H(t_0)) \geq 0. \quad (3)$$

There are two cases:

(1) If at least one of the state variable is not zero, then:

$$\left. \frac{dE}{dt} \right|_{t=t_0} > 0, \tag{4}$$

which is a contradiction similar to (i).

(2) If all state variables are zero, then:

$$\left. \frac{dE}{dt} \right|_{t=t_0} = 0. \tag{5}$$

It is not difficult to show that $E(t) = 0$ for all $t \geq 0$ is the solution with $E(0) = 0$. This is a contradiction to the uniqueness of the solution, since $E(0) > 0$ and $E(t_0) = 0$.

(iii) If $S(t_0) > 0, E(t_0) > 0$ and $N(t_0) = 0$, then:

$$\left. \frac{dN}{dt} \right|_{t=t_0} = \alpha\gamma E(t_0) > 0, \tag{6}$$

which is a contradiction similar to (i).

(iv) If $S(t_0) > 0, E(t_0) > 0, N(t_0) > 0$, and $Y(t_0) = 0$, then:

$$\left. \frac{dY}{dt} \right|_{t=t_0} = \alpha(1 - \gamma)E(t_0) + KN(t_0), \tag{7}$$

which is a contradiction similar to (i). Similarly, $H(t_0) = 0, R(t_0) = 0$, and $V(t_0) = 0$ lead to a contradiction. Thus, $S(t), E(t), Y(t), N(t), H(t), R(t)$ and $V(t)$ are all positive for $t > 0$.

Adding up all equations in (1) and conducting a little algebra yields:

$$\frac{dQ}{dt} + \mu Q \leq A. \tag{8}$$

Its solution $Q(t) \leq \frac{A}{\mu} + \left(N(0) - \frac{A}{\mu}\right)e^{-\mu t}$, since $t \in (0, \infty)$, we have $0 < Q(t) \leq \max\left\{\frac{A}{\mu}, N(0)\right\} = \hat{A}$. Therefore, the set:

$$\Omega = \left\{ (S, E, Y, N, H, R) \in \mathbb{R}_+^6 : 0 \leq S(t) + E(t) + Y(t) + N(t) + H(t) + R(t) + V(t) \leq \hat{A} \right\} \tag{9}$$

is a positively invariant set of system (1). We also note that there is no need to put a restriction on the transmission rate as constant. Instead, it can be a function of time, provided that they are non-negative. \square

Radial Kernels (Functions)

Definition 1. Let Ω be a nonempty arbitrary set. A function $F : \Omega \times \Omega \rightarrow \mathcal{F}$, i.e., \mathbb{R} or \mathbb{C} is called a (real- or complex-valued) kernel on Ω .

If the kernel is real-valued, then the symmetric kernel can be defined. Now, this definition translates $F(\cdot, x_j)$ into trial functions, using certain nodes or $x_1, x_2, \dots, x_N \subset \mathbb{R}^d$. The kernel in the translation-invariant on \mathbb{R}^d can be written as:

$$F(x, y) = \varphi(x, y), \forall (x, y) \in \mathbb{R}^d. \tag{10}$$

One of the most important kernels is the radial kernel, which has important properties. The radial kernel (function) is defined as follows:

Definition 2 ([16–18]). The function $\varphi : \mathbb{R}^d \rightarrow \mathbb{R}$ is radial if a univariate function exists $\Pi : [0, \infty) \rightarrow \mathbb{R}$, such that:

$$\varphi(\mathbf{x}) = \Pi(r), \quad r = \|\mathbf{x}\|_2.$$

using the set of distinct nodal points as $\{\mathbf{x}_1, \mathbf{x}_2, \dots, \mathbf{x}_N\} \subseteq \Omega \subset \mathbb{R}^d$ and the corresponding functions $f_i \in \mathbb{R}$, $i = 1, \dots, N$ for interpolation. We took $S : \mathbb{R}^d \rightarrow \mathbb{R}$ to be a multivariate function. The approximation to S in terms of the radial kernel φ can be given in the following form:

$$S(\mathbf{x}) = \sum_{i=1}^N \lambda_i \varphi(r_i), \tag{11}$$

where $r_i = \|\mathbf{x} - \mathbf{x}_i\|_2$. We now describe how to find the unknown functions λ_i , $i = 1, 2, \dots, N$; using each nodal point in the above (11), we obtained the following system of linear algebraic equations:

$$AY = f, \tag{12}$$

where the coefficient matrix is:

$$A = \begin{bmatrix} \varphi\|\mathbf{x}_1 - \mathbf{x}_1\|_2 & \varphi\|\mathbf{x}_1 - \mathbf{x}_2\|_2 \dots & \varphi\|\mathbf{x}_1 - \mathbf{x}_N\|_2 \\ \varphi\|\mathbf{x}_2 - \mathbf{x}_1\|_2 & \varphi\|\mathbf{x}_2 - \mathbf{x}_2\|_2 \dots & \varphi\|\mathbf{x}_2 - \mathbf{x}_N\|_2 \\ \dots & \dots & \dots \\ \varphi\|\mathbf{x}_N - \mathbf{x}_1\|_2 & \varphi\|\mathbf{x}_N - \mathbf{x}_2\|_2 & \varphi\|\mathbf{x}_N - \mathbf{x}_N\|_2 \end{bmatrix}, \quad Y = \begin{bmatrix} \lambda_1 \\ \lambda_1 \\ \dots \\ \lambda_N \end{bmatrix}, \quad f = \begin{bmatrix} S(\mathbf{x}_1) \\ S(\mathbf{x}_2) \\ \dots \\ S(\mathbf{x}_N) \end{bmatrix}. \tag{13}$$

Once we obtained λ_i , $i = 1, 2, \dots, N$, we substituted it into (11) and obtained an approximate solution of S at the given points. For a unique solution, the system in (12) must be well defined, i.e., the coefficient matrix must be invertible. From [16–18], it is known that if the radial function is strictly positive and definite, this provides invertibility in the coefficient matrix. The definition of a strictly positive property is as follows:

Definition 3 ([18]). A complex-valued continuous even function φ is called a positive definite on \mathbb{R}^d at different given points $\{\mathbf{x}_1, \mathbf{x}_2, \dots, \mathbf{x}_N\} \in \mathbb{R}^d$ if:

$$\sum_{j=1}^N \sum_{i=1}^N \zeta_i \zeta_j \varphi(\mathbf{x}_i - \mathbf{x}_j) \geq 0, \quad \zeta = [\zeta_1, \dots, \zeta_N]. \tag{14}$$

Moreover, the function is called a strictly positive definite on \mathbb{R}^d if the quadratic form (15) is zero only for $\zeta \equiv 0$. Some of the most common RBFs (radial base functions) are the following:

- The Gaussian (GA): $\varphi(r) = \exp(-(\epsilon r)^2)$;
- The Laguerre–Gaussian (LG): $\varphi(r) = (2 - r^2) \exp(-r^2)$;
- The inverse quadratic (IQ): $\varphi(r) = \frac{1}{(\epsilon r)^2 + 1}$;
- The generalized inverse multiquadric (GIMQ): $\varphi(r) = \frac{1}{((\epsilon r)^2 + 1)^{\frac{i}{2}}}$, $i = 1, 2, \dots$

Amongst these, the Gaussian is the most popular function because it has attractive mathematical properties, and its hill-like shape is easy to control with parameter σ .

4. Forced SEYNHRV-S Model

The prevention measures and variants of COVID-19 cause changes in the value of the transmission rate ($\beta_i, i = 1, 2$ and 3) and possibly the other parameters involved in the modeling; moreover, the COVID-19 pandemic data show more than one wave, which indicates that the transmission rates must be represented as a function of time. Herein, we considered the forced SEYNHRV-S model, where the infection rates are a function of time. The model parameters are defined here as piecewise constants, except for the transmission rate, which is a continuous function of time that made our model fit COVID-19 data. In the literature, there are several forms of transmission rates [19]. In this study, since we only had data for the symptomatic population, we showed that the transmission rate for the symptomatic population can be represented as a linear combination of the Gaussian radial function:

$$\beta_1(t) = \sum_{i=1}^n c_i \exp(-\sigma_i(t - t_i)^2), t \in [0, \infty). \tag{15}$$

In [20], the authors considered exactly the same equation in terms of statistical tools, whereas we used real COVID-19 data from Saudi Arabia. We first smoothed the given data and used the nonlinear differential equation, derived below in Equation (17), and we showed that our numerical solution can be represented in the form of Equation (15). This is the main difference between the work here and the approach in [20]. In this study, we provide mathematical proof and also assume that $\beta_2(t) \approx \beta_2^0$ and $\beta_3(t) \approx \beta_3^0$. Table 1 indicates the list of parameters used in this study.

Table 1. Model parameters used in our model and their respective definitions.

Parameter	Description	Reported Value	Experimental Value
β_2^0	Transmission rate of the asymptomatic population	$(1 \times 10^8, 2 \times 10^6)$	$(0, 0.025)$
β_3^0	Transmission rate of the hospitalized population	$(1 \times 10^9, 2 \times 10^7)$	$(0, 0.0025)$
μ		Natural death rate 3.6593×10^{-5} (Saudi Arabia)	
α	Incubation period	$(1/14, 1/21)$	$(1/8, 1/6)$
γ	Fraction of the individuals ultimately becoming infected		
$1/\Phi_Y$	Mean symptomatic infectious period	$(14, 21)$	$(8, 16)$
$1/\Phi_N$	Mean symptomatic infectious period	$(14, 21)$	$(8, 16)$
ν	Vaccination rate—data taken from Saudi Arabia		
ψ	Rate of recovered individuals losing their immunity and returning to S		
ϵ	Rate of symptomatic individuals becoming hospitalized	$(0.1, 0.5)$	$(0.01, 1)$
K	Rate of asymptomatic individuals becoming symptomatic	$(0.05, 0.5)$	$(0.01, 1)$
r	Rate of recovered individuals becoming hospitalized patients	$(0.05, 0.5)$	$(0.01, 1)$
μ_2	Death rate of hospitalized patients	$(0.05, 0.5)$	$(0.01, 1)$

Driving the Transmission Rate from the Infected Population and a Numerical Solution

Since we only had data for current symptomatic population cases and $\eta = 0$ throughout this study, nonzero cases were investigated, and we could reduce the system in Equation (1) to a simpler form:

$$\left. \begin{aligned} \frac{dS}{dt} &= A - \beta_1(t)YS - (\mu + \nu)S, \\ \frac{dE}{dt} &= \beta_1(t)YS - (\alpha + \mu)E, \\ \frac{dY}{dt} &= \alpha E - (\Phi_Y + \varepsilon + \mu_1 + \mu)Y. \end{aligned} \right\} \tag{16}$$

Since $E(t) \geq 0$, we should have $\frac{dY}{dt} + (\Phi_Y + \varepsilon + \mu_1 + \mu)Y > 0$, and since $\beta_1(t)YS > 0$, we should have $\frac{dE}{dt} + (\alpha + \mu)E > 0$, or using the last equation of the system above, we can obtain $\frac{d^2Y(t)}{dt^2} + (\alpha + \mu + \pi)\frac{dY(t)}{dt} + \pi(\mu + \alpha)Y(t) > 0$.

After lengthy but straightforward calculations, solving $S(t)$ from the second equation of Equation (16), and substituting it into one of the above equations in Equation (16), we found (as in [21]) that:

$$M(Y(t))\frac{d\beta_1(t)}{dt} + N(Y(t))\beta_1^2(t) + P(Y(t))\beta_1(t) = 0. \tag{17}$$

This is the Bernoulli differential equation, where:

$$M(Y(t)) = -\frac{Y(t)}{\alpha} \left(\frac{d^2Y(t)}{dt^2} + (\alpha + \mu + \pi)\frac{dY(t)}{dt} + \pi(\mu + \alpha)Y(t) \right), \quad N(Y(t)) = -Y(t)M(Y(t)) - A\alpha Y^2(t), \tag{18}$$

$$P(Y(t)) = -M(Y(t))(\mu + \nu) + \frac{Y(t)}{\alpha} \left((\alpha + \mu + \pi)\frac{d^2Y(t)}{dt^2} + \frac{d^3Y(t)}{dt^3} \right) - \frac{1}{\alpha} \left((\alpha + \mu + \pi) \left(\frac{dY(t)}{dt} \right)^2 + \frac{dY(t)}{dt} \frac{d^2Y(t)}{dt^2} \right)$$

and:

$$\pi = \Phi_Y + \varepsilon + \mu_1 + \mu$$

Theorem 2. For a given positive function $f(t)$, $\pi > 0$, $\alpha > 0$, $\mu > 0$, $\nu > 0$, $\beta_{10} > 0$ and $T > 0$, $K > 0$ exists, such that if $\beta_{10} < K$, there is the solution $\beta_1(t)$ with $\beta_1(0) = \beta_{10}$, such that $Y(t) = f(t)$ for $0 < t \leq T$ if (and only if) $\frac{df}{dt} + (\Phi_Y + \varepsilon + \mu_1 + \mu)f > 0$ and $\frac{d^2f(t)}{dt^2} + (\alpha + \mu + \pi)\frac{df(t)}{dt} + \pi(\mu + \alpha)f(t) > 0$. This solution is also unique (see, for example, [20]).

Since an analytical solution was not possible, we needed a numerical method to solve Equation (17); here, we used the finite difference technique. We then tried to compute a grid function consisting of the values X_1, X_2, \dots, X_m , where X_i is our approximation to the solution $1/\beta_1(t_i)$; here, $t_i = ih$ and $h = t_{i+1} - t_i$ is the step size, and we used the centered finite difference to approximate $\frac{dY(t)}{dt}$, $\frac{d^2Y(t)}{dt^2}$ and $\frac{d^3Y(t)}{dt^3}$. We replaced $\frac{dY(t)}{dt}$, $\frac{d\beta_1(t)}{dt}$, $\frac{d^2Y(t)}{dt^2}$, and $\frac{d^3Y(t)}{dt^3}$ with the centered finite difference approximation:

$$Dy_j = \frac{y_{j+1} - y_{j-1}}{2h}, \quad D^2y_j = \frac{y_{j+1} - 2y_j + y_{j-1}}{h^2}, \quad D^3y_j = \frac{y_{j+2} - 2y_{j+1} + 2y_{j-1} - y_{j-2}}{2h^3},$$

and $\frac{dX(t)}{dt}$ with forward difference approximation:

$$DX_i = \frac{X_{i+1} - X_i}{h}$$

We then obtained following the algebraic equations after changing the dependent variable from the nonlinear differential Equation (17):

$$\begin{aligned}
 & \frac{-y_i}{\alpha} [(-2 + \pi(\tau + \alpha))y_i + (1 - \frac{1}{2}\alpha - \frac{1}{2}\tau - \frac{1}{2}\pi)y_{i-1} \\
 & + (1 + \frac{1}{2}\alpha + \frac{1}{2}\tau + \frac{1}{2}\pi)y_{i+1}](X_{i+1} - X_i) \\
 & + \frac{y_i^2}{\alpha} [(-2 + \pi(\tau + \alpha))y_i + (1 - \frac{1}{2}\alpha - \frac{1}{2}\tau - \frac{1}{2}\pi)y_{i-1} \\
 & + (1 + \frac{1}{2}\alpha + \frac{1}{2}\tau + \frac{1}{2}\pi)y_{i+1} - A\alpha] + \left[\frac{1}{\alpha} \left(-\frac{\tau}{4} - \frac{\pi}{4} + \frac{1}{2} - \frac{\alpha}{4} \right) y_i^2 \right. \\
 & + \left(\frac{1}{\alpha} \left(\frac{\tau}{2} + \frac{\pi}{2} + \frac{\alpha}{2} \right) y_{i+1} + \left(-\frac{\tau}{2} - \frac{\pi}{2\alpha} + 1 - \frac{\tau^2}{2\alpha} + \frac{2\tau}{\alpha} + \frac{\pi}{\alpha} \right) y_i \right) y_{i-1} \\
 & + \frac{1}{\alpha} \left(-\frac{\tau}{4} - \frac{\pi}{4} - \frac{1}{2} - \frac{\alpha}{4} \right) y_{i+1}^2 + \left(\frac{\tau}{2} + \frac{\pi}{2\alpha} + 1 + \frac{\tau^2}{2\alpha} + \frac{2\tau}{\alpha} + \frac{\pi}{\alpha} \right) y_i y_{i+1} + (\tau\pi - 2 \\
 & + \frac{\tau^2\pi}{2\alpha} - \frac{4\tau}{\alpha} - \frac{2\pi}{\alpha}) y_i^2 + \frac{1}{2\alpha} (y_{i+2} - y_{i-2}) y_i \Big] X_i = 0, i \\
 & = 1, \dots, N,
 \end{aligned} \tag{19}$$

where $X(t) = \frac{1}{\beta_1(t)}$. We used the data provided by the Ministry of Health in Saudi Arabia for daily infection cases. Mathematically, there are infinite choices of $X(0) = \frac{1}{\beta_1(0)}$, and we used some well-known values [22].

We can give the stability and convergence of the Euler method for a numerical solution of Equation (17) using the following theorem. First, after changing the dependent variable to $x(t) = \frac{1}{\beta_1(t)}$, the resulting equation can be written in a more compact form:

$$\frac{dx(t)}{dt} = f \left(Y(t), \frac{dY(t)}{dt}, \frac{d^2Y(t)}{dt^2}, \frac{d^3Y(t)}{dt^3}, x(t) \right), \quad x(t_0) = \frac{1}{\beta_1(0)}, \tag{20}$$

Additionally, utilizing the above finite differences in Equation (5), we can obtain:

$$\begin{aligned}
 x_{j+1} = x_j + hf & \left(Y_j, \frac{Y_{j+1} - Y_{j-1}}{2h} + O(h^2), \frac{Y_{j+1} - 2Y_j + Y_{j-1}}{h^2} \right. \\
 & \left. + O(h^2), \frac{Y_{j+2} - 2Y_{j+1} + 2Y_{j-1} - Y_{j-2}}{2h^3} + O(h^2), x_j \right) + \frac{h^2}{2} x''(\xi_j)
 \end{aligned}$$

If we drop all of the terms with orders of h^2 and higher, we can obtain:

$$X_{j+1} = X_j + h\varphi \left(y_j, \frac{y_{j+1} - y_{j-1}}{2h}, \frac{y(t_{i+1}) - 2y(t_i) + y(t_{i-1}))}{h^2}, \frac{y(t_{i+2}) - 2y(t_{i+1}) + 2y(t_{i-1}) - y(t_{i-2}))}{2h^3}, X_j \right), \quad X(t_0) = X_0 = \frac{1}{\beta_1(0)}.$$

Theorem 3. Suppose the initial-valued problem:

$$\frac{dx(t)}{dt} = f \left(Y(t), \frac{dY(t)}{dt}, \frac{d^2Y(t)}{dt^2}, \frac{d^3Y(t)}{dt^3}, x(t) \right), \quad x(t_0) = \frac{1}{\beta_1(0)}, \tag{21}$$

is approximated by a one-step method in the form of:

$$x_{j+1} = x_j + h\varphi \left(y_j, \frac{y_{j+1} - y_{j-1}}{2h}, \frac{y(t_{i+1}) - 2y(t_i) + y(t_{i-1}))}{h^2}, \frac{y(t_{i+2}) - 2y(t_{i+1}) + 2y(t_{i-1}) - y(t_{i-2}))}{2h^3}, X_j \right).$$

Assume that $\varphi \left(X, h, y(t), \frac{dy(t)}{dt}, \frac{d^2y(t)}{dt^2}, \frac{d^3y(t)}{dt^3} \right)$ is continuous and satisfies the Lipschitz condition in variable X with the Lipschitz constant K on the set:

$$D = \{ (t, X, h) : a \leq t \leq b \text{ and } -\infty < X < \infty, 0 \leq h \leq h_0 \}. \tag{22}$$

Then:

- (i) The method is stable;
- (ii) The differences method is convergent if it is equivalent to $\varphi\left(X, h, y(t), \frac{dy(t)}{dt}, \frac{d^2y(t)}{dt^2}, \frac{d^3y(t)}{dt^3}\right) = f\left(x, Y(t), \frac{dY(t)}{dt}, \frac{d^2Y(t)}{dt^2}, \frac{d^3Y(t)}{dt^3}\right)$ for all $a \leq t \leq b$;
- (iii) If the ζ function of h exists, then for each, $j = 1, 2, \dots, N$, the local truncation error $\zeta_i(h)$ satisfies $|\zeta_j(h)| \leq \zeta(h)$ whenever $0 \leq h \leq h_0$, then:

$$|x(t_j) - X_j| \leq \frac{\zeta(h)}{L} e^{L(t_j-a)}$$

Proof. See, for example, Gear’s book [23] (pp. 57–58). We also note that after four steps, we also used the fourth-order Adams–Bashforth technique and compared the results of both methods. We found no significant difference between the two methods. □

5. Methodology

Saudi Arabia has a population of over 34 million people, and non-Saudis form approximately 37% of the total population. Saudi Arabia has a well-established and advanced healthcare system that is offered for free to all residents, and Saudi Arabia might have been one of the first countries that took early actions to prevent and control the spread of COVID-19.

The Saudi Ministry of Health (MOH) publishes daily COVID-19 data that include the number of total cases, recoveries, mortalities, critical cases, and active cases. It also provides free doses of the COVID-19 vaccine and conducts daily examinations.

Model Calibration

We adopted a similar approach to [22] for model calibration and to adjust our model parameters. Parameters such as recovery rates ($1/\Phi_Y, 1/\Phi_N$) and the incubation period (α) are well studied in the literature, so we aimed to calibrate the parameters that are not readily available in previous works (such as $\beta_1(t), \beta_2(t),$ and $\beta_3(t)$) or that are unique to our presented model. We also included variables that are more sensitive to the output variable, such as γ . Since there are no available data to estimate $\beta_2(t)$ and $\beta_3(t)$, we assumed that they were constant. Finding the transmission rate $\beta_1(t)$ for the symptomatic population was carried out as explained above.

6. Results

Based on laboratory data published in [22], the population of asymptomatic individuals is much higher than that estimated before, with the average SAR-CoV-2-positive infection rate being more than ten times the reported value. To examine different theories of the spread of COVID-19 and to validate their possibilities, we tried to capture the curvature of the line representing the reported number of infections as much as possible. This was achieved by introducing the new technique described above. From Equation (1), the ratio between the symptomatic and asymptomatic populations is dictated by:

$$\frac{Y}{N} = \frac{\alpha(1 - \gamma)}{\alpha\gamma} = \frac{1}{\gamma} - 1. \tag{23}$$

The selection of value γ is important, and our meaningful results suggest that the asymptomatic population is a third of the symptomatic population, which support the findings in [22].

One of the most critically important parameters that affects compartmental modeling is the initial susceptible population, $S(0)$. What makes the COVID-19 pandemic unique is the abundance of information and public awareness about this virus. When the first infections in many communities were encountered, a significant portion of the population was already on high alert and practiced self-isolation. Thus, the initial susceptible population must be investigated in detail.

Since we only had data for symptomatic cases, we derived the transmission rate $B(t)$ for the symptomatic population. We first solved Equation (18) to obtain the transmission rate $B(t)$, where we used the COVID-19 data of Saudi Arabia, after using the exponential smoothing technique. The total numbers of COVID-19 and active cases are given in Figure 2a,b. The data in Figure 2a were used in Equation (19), and we solved Equation (19) for $B_i, i = 1, 2, \dots, N$. We found that the transmission rate $B(t)$ increased in the first 10 days and reached the maximum value on day 10, and then greatly decreased during the first 40 days, as seen in Figure 3. After 40 days, we saw oscillation and a decrease in the value of the transmission rate $B(t)$ until 320 days (see Figure 4). We then suddenly found an increase in the value of the transmission rate $B(t)$, which reached a peak point at around 350 days. After that, the transmission rate began to decrease until day 370, after which it formed another peak at around 405 days (see Figure 4). From this day and on, the transmission rate $B(t)$ decreased with small oscillations (see Figure 5). The previously mentioned figures show that the transmission rate $B(t)$ is not constant, but it is rather a complex function of time. This comprehensive and elegant numerical solution has not been given before. Of course, we can use numerical values of the transmission rate [24] in our model (Equation (1)) to obtain numerical solutions, which will be undertaken in our forthcoming paper. In this study, we explored the radial function to fit the discrete values of the transmission rate, which was obtained from our numerical solution of the transmission rate $B(t)$. It is extremely important to obtain analytical approximation, because other researchers can readily use it. After examining all possibilities in Definition 3, we found that the linear combination of the Gaussian radial function is more suitable than the others to represent the numerical values of the transmission rate $B(t)$. We need a simple yet effective representation of the transmission rate function. We can write large a number of linear combinations of the Gaussian radial function and can obtain the constant to fit the numerical results, which will provide a satisfactory small error, as stated earlier. We need a simple analytical representation for the transmission rate $B(t)$. We carried out such an approximation for the transmission rate $B(t)$ as follows:

$$\beta_1(t) \approx B(t) = 6.35555554 \cdot 10^{-8} \left(1 + 5e^{-0.01(t-10)^2} + 0.3e^{-0.001(t-350)^2} + 0.48e^{-0.001(t-450)^2} \right), \tag{24}$$

$$\beta_0(t) \approx 9.35555554 \cdot 10^{-8},$$

which can be seen in Figure 6b. When comparing the actual and numerical values, we can see a similar structure in Figure 6a. We compared the prediction of the model with the constant transmission rate and the other models, where the transmission rate was a function of time. The function $(\beta_1(t))$ was a linear combination of the Gaussian radial function and the real published COVID-19 data of Saudi Arabia, where the value of the other parameters involved in the modeling were the same as before. Figure 7 shows the active COVID-19 cases of Saudi Arabia, where the asterisks represent the real data, and the continuous line represents the model prediction for the current active cases for symptomatic individuals. Since the government of Saudi Arabia implemented many rules to prevent the spread of COVID-19, such as a lockdown for almost three months, a strict curfew, the requirement of wearing face masks, and social distancing, these must be taken into account for the initial suspected population. Because of these reasons, we took the initial susceptible population as $S(0) = \frac{3418169}{5}$ and $\nu = 0.0025$, so that after 300 days, approximately 75% of the total population became vaccinated. Figure 8 shows the model prediction of the symptomatic, asymptomatic, and hospitalized population evaluation with time, where the continuous, dashed, and dashed/dotted lines represent the current active cases for symptomatic, asymptomatic, and hospitalized individuals, respectively. We can also see a second wave for the current active cases of the asymptomatic and hospitalized populations as expected, where the time-dependent transmission rate $B(t)$ for the symptomatic population is taken as:

$$\beta_1(t) \approx B(t) = 6.35555554 \cdot 10^{-8} \left(1 + 5e^{-0.01(t-10)^2} + 3e^{-0.001(t-350)^2} + 4.8e^{-0.001(t-450)^2} \right). \tag{25}$$

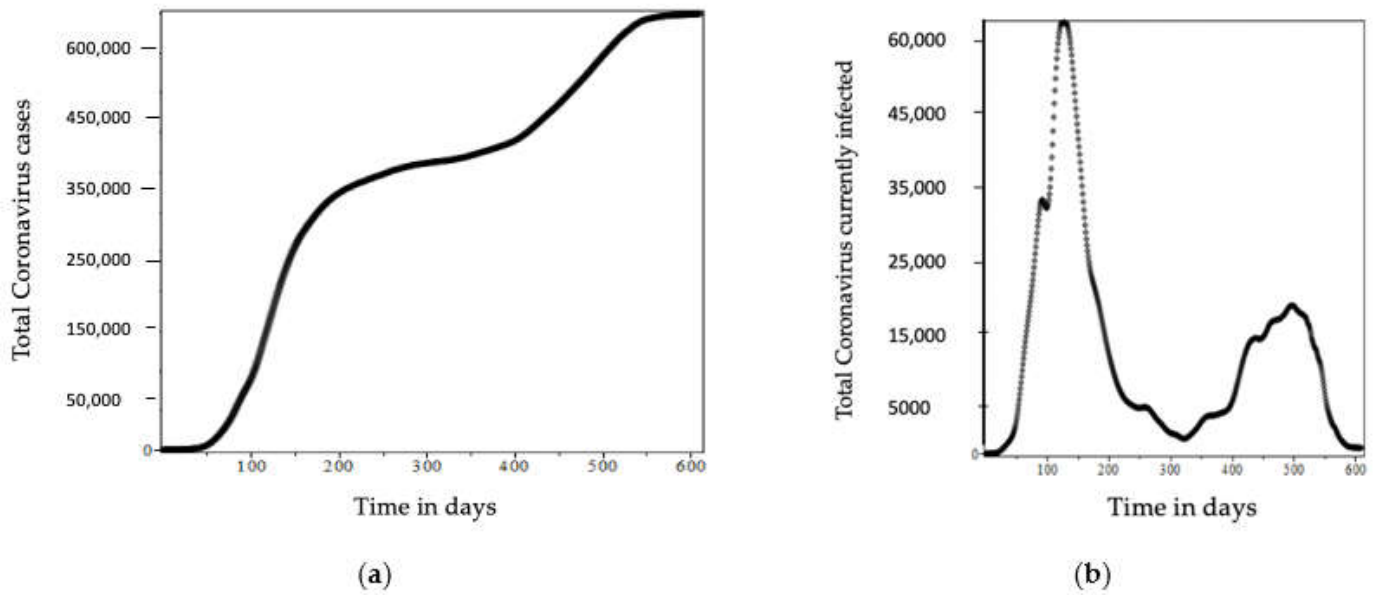


Figure 2. (a) Total COVID-19 cases in Saudi Arabia. (b) Current active cases in Saudi Arabia (<https://www.worldometers.info/coronavirus/country/saudi-arabia/> accessed on 18 December 2021).

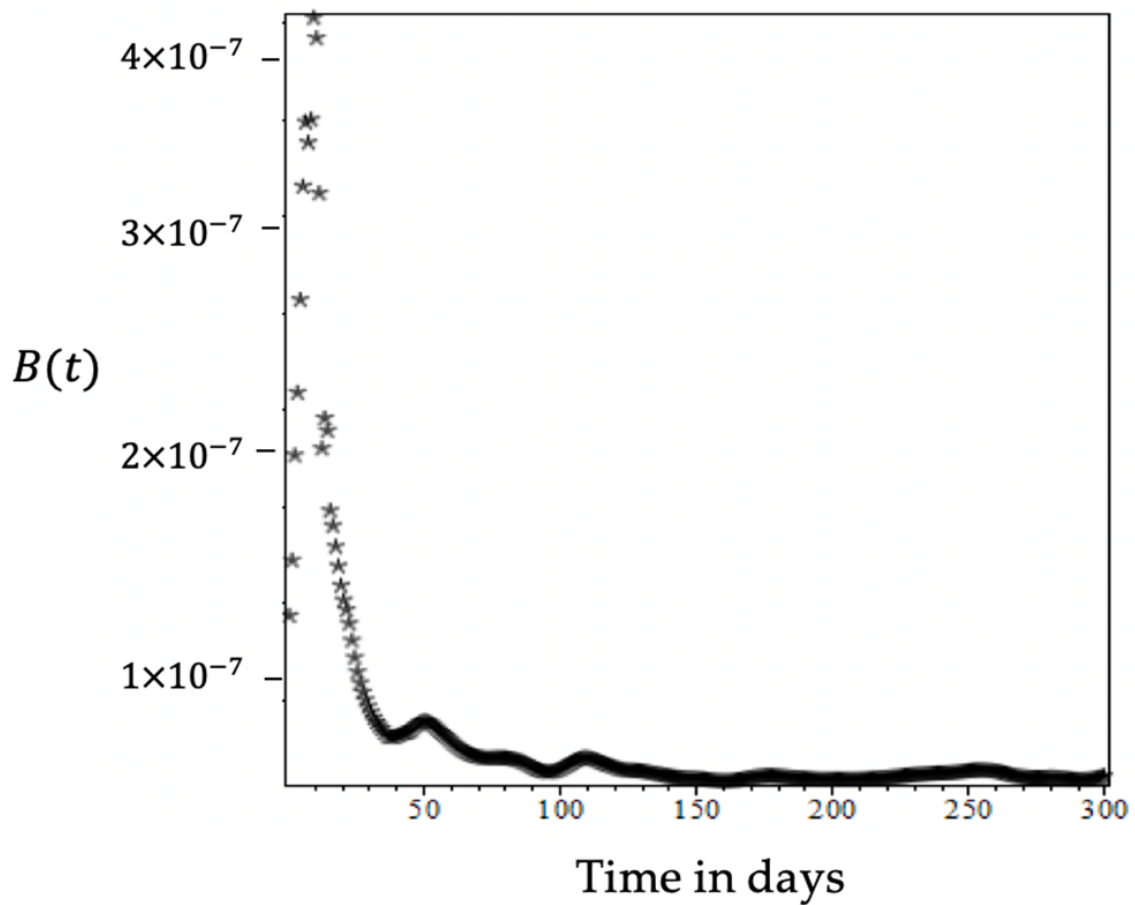


Figure 3. Time development of the transmission rate of the symptomatic population, $0 \leq t \leq 300$.

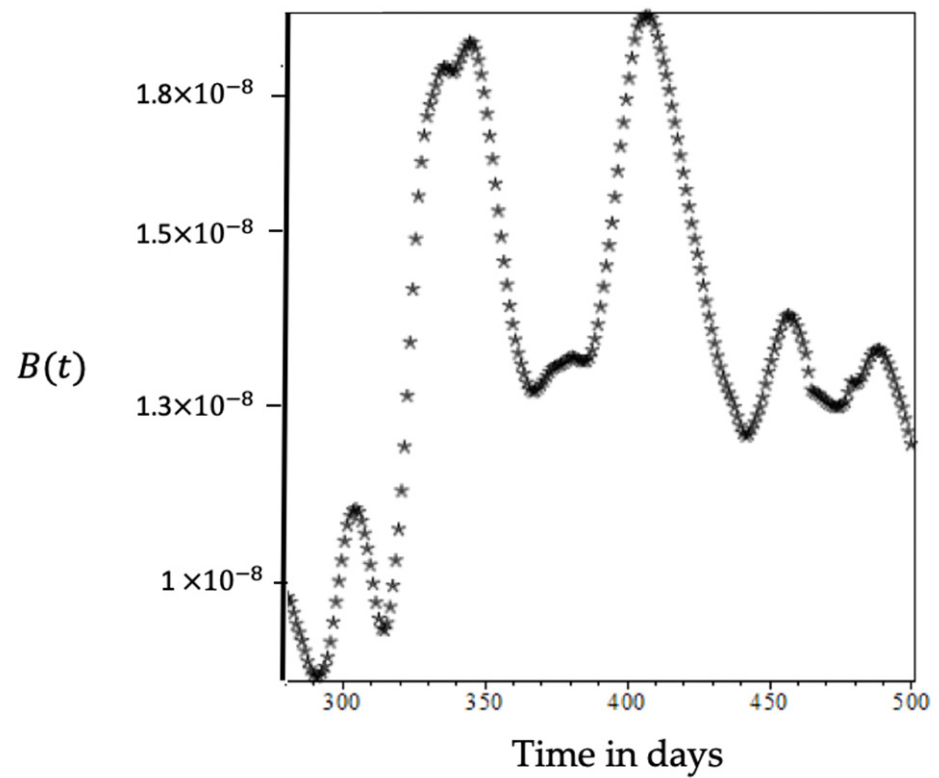


Figure 4. Time development of the transmission rate of the symptomatic population, $270 \leq t \leq 500$.

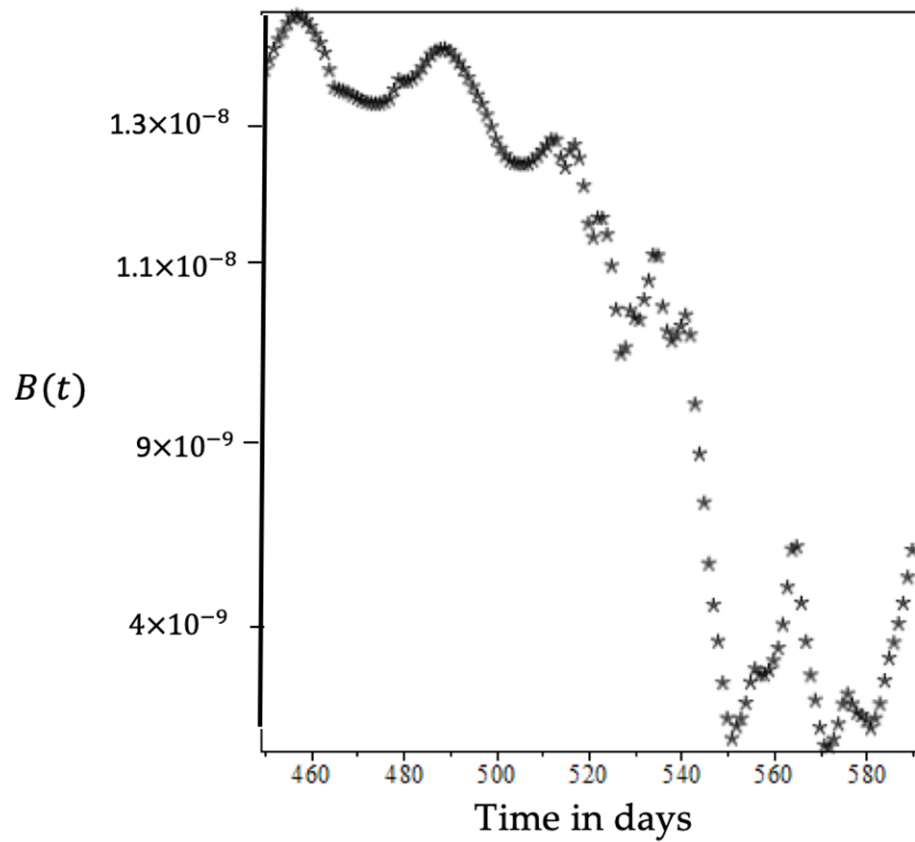


Figure 5. Time development of the transmission rate of the symptomatic population, $450 \leq t < 600$.

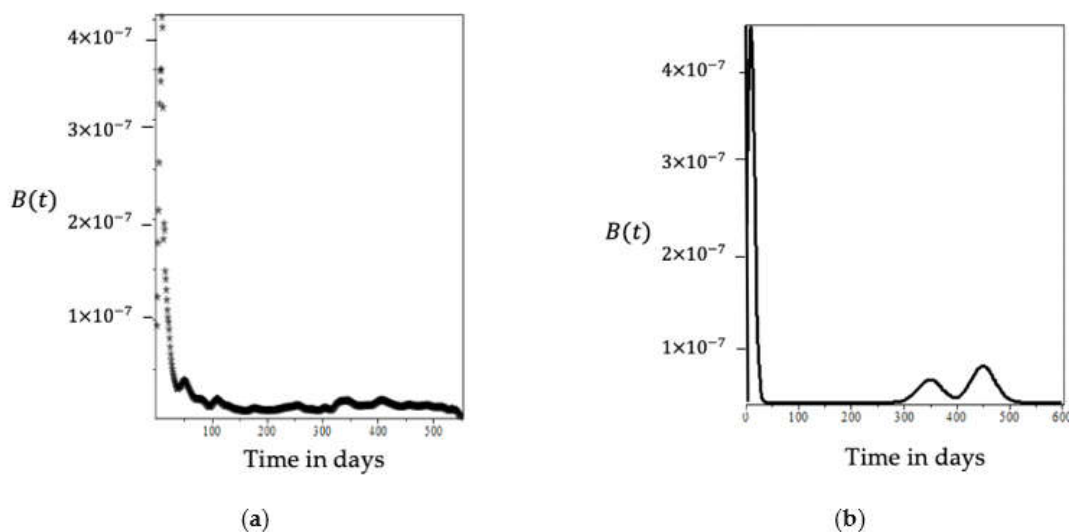


Figure 6. Time development of the transmission rate for the symptomatic population: (a) numerical results; (b) approximation by linear combinations of Gaussian radial functions.

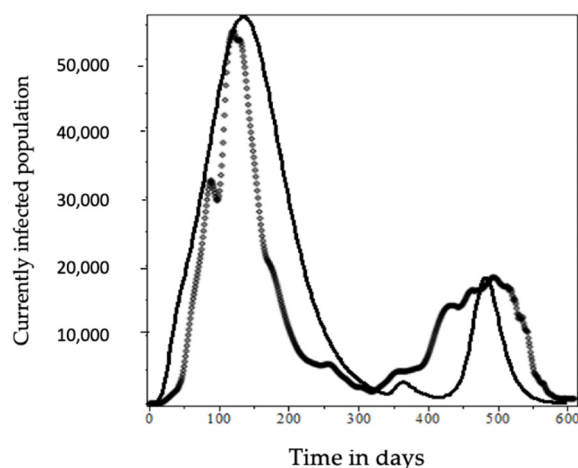


Figure 7. Current active cases in Saudi Arabia. Asterisks represent the real data, and the continuous line ($Y(t)$) represents the model prediction.

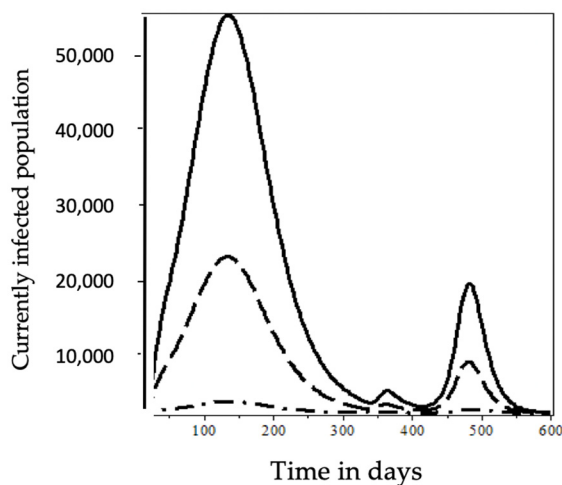


Figure 8. Model prediction of the current active cases in the Saudi Arabia: continuous line ($Y(t)$), dashed line ($N(t)$), and dashed/dotted line ($H(t)$).

This is exactly in the form of Equation (22), where the only difference is that the second and third Gaussian radial functions were multiplied by 10. Of course, we could find a better approximation if we used more Gaussian radial functions, but we wanted to use the derived transmission rate function from the real COVID-19 data. We now assumed that $\beta_1(t) = 6.35555554 \cdot 10^{-8}$ is a constant and all parameters were the same as before, and we compared the model prediction with real COVID-19 data, as in Figure 9. We can see that those compartmental models with constant parameters cannot be used to model the COVID-19 epidemic. Let us now examine the effect of vaccination on the spread of COVID-19 disease. Figures 10 and 11 were generated with the same parameters as in Figures 7 and 8, except the vaccination rate ($v = 0$). Figures 10 and 11 represent the time development of the suspected, recovered, symptomatic, asymptomatic, and hospitalized populations, respectively. Figure 11 shows that the effect of the COVID-19 pandemic would have been much more severe without vaccination.

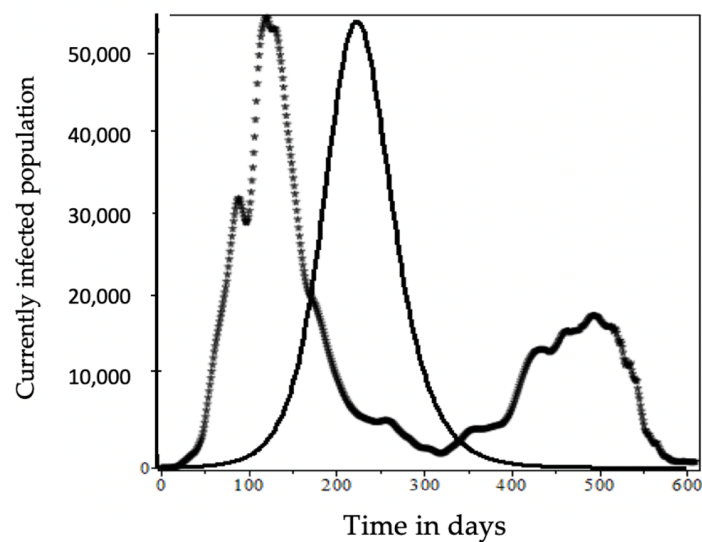


Figure 9. Current active cases in Saudi Arabia. Asterisks represent the real data, and the continuous line ($Y(t)$) represents the model prediction with a constant transmission rate for the symptomatic population.

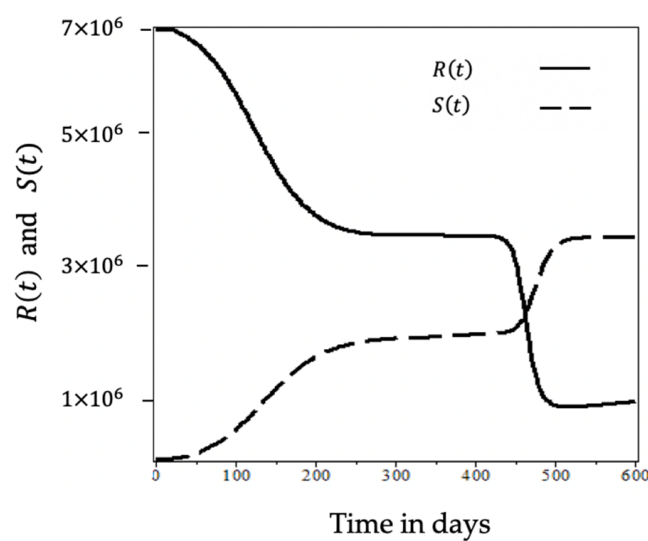


Figure 10. Development of the number of suspected $S(t)$ and recovered $R(t)$ individuals with time without vaccination.

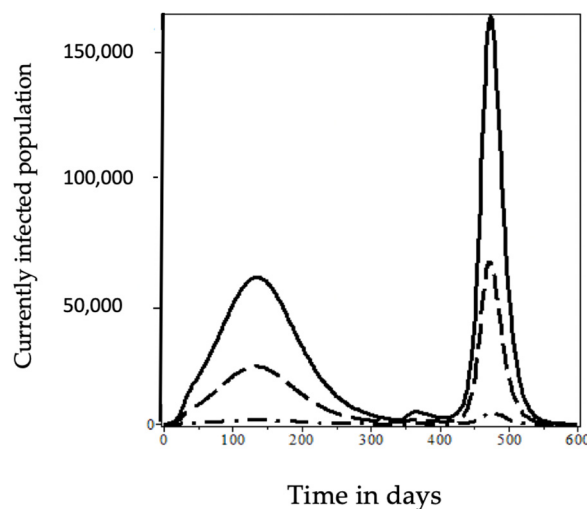


Figure 11. Model prediction of current active cases without vaccination: continuous line $Y(t)$, dashed line $N(t)$, and dashed/dotted line $H(t)$.

7. Discussion

We presented a new technique to compute the time-dependent transmission rate from the published COVID-19 data from Saudi Arabia. To obtain the best optimized initial value $\beta_1(0)$, we ran our model with a constant coefficient several times for several constants β_1 ; we then selected the best suitable value as the initial value of the transmission rate. Recently, Pollicott et al. [21] derived the same nonlinear differential functions; they tried to represent the discrete data using analytical functions, but it is well known that one can use any orthogonal function or polynomial approach given the discrete data within the required error. One can also increase the number of orthogonal polynomials or the degree of polynomials if necessary. The technique they used was not suitable for COVID-19 data; instead, we approached each derivative using the finite difference technique, and in this way, we obtained novel results.

The crucial part of this paper showed that we can approach discrete values of the transmission rate in terms of linear combinations of Gaussian radial functions; we then ran our model to show the second wave as seen in real data.

Author Contributions: Conceptualization, F.S.A. and E.A.T.; methodology, F.S.A. and E.A.T.; software, F.S.A. and E.A.T.; validation, F.S.A. and E.A.T.; formal analysis, F.S.A. and E.A.T.; investigation, F.S.A. and E.A.T.; resources, F.S.A. and E.A.T.; data curation, F.S.A. and E.A.T.; writing—original draft preparation, F.S.A. and E.A.T.; writing—review and editing, F.S.A.; visualization, F.S.A. and E.A.T. All authors have read and agreed to the published version of the manuscript.

Funding: This research was funded by the Deanship of Scientific Research at Imam Mohammad Ibn Saud Islamic University through Research Group no. RG-21-09-16.

Institutional Review Board Statement: Not applicable.

Informed Consent Statement: Not applicable.

Data Availability Statement: The authors confirm that the data supporting the findings of this study are available within the article.

Acknowledgments: The authors extend their appreciation to the Deanship of Scientific Research at Imam Mohammad Ibn Saud Islamic University for funding this work through Research Group no. RG-21-09-16.

Conflicts of Interest: The authors declare no conflict of interest.

References

1. WHO. Coronavirus Disease (COVID-19) Pandemic. Available online: <https://www.who.int/emergencies/diseases/novel-coronavirus-2019> (accessed on 17 November 2021).
2. Cao, L.; Liu, Q. COVID-19 Modeling: A Review. *arXiv* **2021**, arXiv:2104.12556. Available online: <https://arxiv.org/abs/2104.12556> (accessed on 3 November 2021).
3. Kermack, W.O.; McKendrick, A.G. A contribution to the mathematical theory of epidemics. *Proc. R. Soc. A* **1927**, *115*, 700–721.
4. Ivorra, B.; Ferrández, M.R.; Vela-Pérez, M.; Ramos, A.M. Mathematical modeling of the spread of the coronavirus disease 2019 (COVID-19) taking into account the undetected infections. The case of China. *Commun. Nonlinear Sci. Numer. Simul.* **2020**, *88*, 105303. [[CrossRef](#)] [[PubMed](#)]
5. Giordano, G.; Colaneri, M.; Di Filippo, A.; Blanchini, F.; Bolzern, P.; Nicolao, G.D.; Sacchi, P.; Colaneri, P.; Bruno, R. Modeling vaccination rollouts, SARS-CoV-2 variants and the requirement for non-pharmaceutical interventions in Italy. *Nat. Med.* **2021**, *27*, 993–998. [[CrossRef](#)] [[PubMed](#)]
6. Antonini, C.; Calandrini, S.; Bianconi, F. A Modeling Study on Vaccination and Spread of SARS-CoV-2 Variants in Italy. *Vaccine* **2021**, *9*, 915. [[CrossRef](#)] [[PubMed](#)]
7. Yang, H.M.; Lombardi, L.S., Jr.; Castro, F.F.M.; Yang, A.C. Mathematical modeling of the transmission of SARS-CoV-2—Evaluating the impact of isolation in São Paulo State (Brazil) and lockdown in Spain associated with protective measures on the epidemic of COVID-19. *PLoS ONE* **2021**, *16*, e0252271. [[CrossRef](#)] [[PubMed](#)]
8. Ramos, M.R.; Vela-Pérez, A.M.; Ferrández, M.; Kubik, A.B.; Ivorra, B. Modeling the impact of SARS-CoV-2 variants and vaccines on the spread of COVID-19. *Commun. Nonlinear Sci. Numer. Simul.* **2021**, *102*, 105937. [[CrossRef](#)] [[PubMed](#)]
9. Moore, S.; Hill, E.M.; Tildesley, M.J.; Dyson, L.; Keeling, M.J. Vaccination and non-pharmaceutical interventions for COVID-19: A mathematical modelling study. *Lancet Infect. Dis.* **2021**, *21*, 793–802. [[CrossRef](#)]
10. Mancuso, M.; Eikenberry, S.E.; Gumel, A.B. Will Vaccine-Derived Protective Immunity Curtail COVID-19 Variants in the US? *Infect. Dis. Model.* **2021**, *6*, 1110–1134. [[CrossRef](#)] [[PubMed](#)]
11. Ngonghala, C.N.; Knitter, J.R.; Marinacci, L.; Bonds, M.H.; Gumel, A.B. Assessing the impact of widespread respirator use in curtailing COVID-19 transmission in the USA. *R. Soc. Open Sci.* **2021**, *8*, 210699. [[CrossRef](#)] [[PubMed](#)]
12. Asamoah, J.K.K.; Jin, Z.; Sun, G.-Q.; Seidu, B.; Yankson, E.; Abidemi, A.; Oduro, F.; Moore, S.E.; Okyere, E. Sensitivity assessment and optimal economic evaluation of a new COVID-19 compartmental epidemic model with control interventions. *Chaos Solitons Fractals* **2021**, *146*, 110885. [[CrossRef](#)] [[PubMed](#)]
13. Asamoah, J.K.K.; Owusu, M.A.; Jin, Z.; Oduro, F.; Abidemi, A.; Gyasi, E.O. Global stability and cost-effectiveness analysis of COVID-19 considering the impact of the environment: Using data from Ghana. *Chaos Solitons Fractals* **2020**, *140*, 110103. [[CrossRef](#)] [[PubMed](#)]
14. Demongeot, J.; Flet-Berliac, Y.; Seligmann, H. Temperature decreases spread parameters of the new COVID-19 case dynamics. *Biology* **2020**, *9*, 94. [[CrossRef](#)] [[PubMed](#)]
15. Alshammari, F.S. A Mathematical Model to Investigate the Transmission of COVID-19 in the Kingdom of Saudi Arabia. *Comput. Math. Methods Med.* **2020**, *2020*, 9136157. [[CrossRef](#)] [[PubMed](#)]
16. Buhmann, M.D. Radial basis functions: Theory and implementations. In *Cambridge Monographs on Applied and Computational Mathematics*; Cambridge University Press: Cambridge, UK, 2003; Volume 12.
17. Wendland, H. Scattered Data Approximation. In *Cambridge Monographs on Applied and Computational Mathematics*; Cambridge University Press: Cambridge, UK, 2005.
18. Schaback, R. A Practical Guide to Radial Basis Functions. 2007. Available online: num.math.uni-goettingen.de/schaback/teaching/sc.pdf (accessed on 8 December 2021).
19. Chalkiadakis, I.; Yan, H.; Peters, G.W.; Shevchenko, P.V. Infection rate models for COVID-19: Model risk and public health news sentiment exposure adjustments. *PLoS ONE* **2021**, *16*, e0253381. [[CrossRef](#)]
20. Corsaro, C.; Sturniolo, A.; Fazio, E. Gaussian Parameters Correlate with the Spread of COVID-19 Pandemic: The Italian Case. *Appl. Sci.* **2021**, *11*, 6119. [[CrossRef](#)]
21. Pollicott, M.; Wang, H.; Weiss, H. Extracting the time dependent transmission rate from infection data via solution of an inverse ODE problem. *J. Biol. Dyn.* **2012**, *6*, 509–523. [[CrossRef](#)] [[PubMed](#)]
22. Ramezani, S.B.; Amirlatifi, A.; Rahimi, S. A novel compartmental model to capture the nonlinear trend of COVID-19. *Comput. Biol. Med.* **2021**, *134*, 104421. [[CrossRef](#)] [[PubMed](#)]
23. Gear, C.W. *Numerical Initial-Value Problems in Ordinary Differential Equations*; Prentice-Hall: Englewood Cliffs, NJ, USA, 1971; Volume 253, pp. 57–58.
24. General Authority of Statistics, Kingdom of Saudi Arabia. Available online: <https://www.stats.gov.sa/en> (accessed on 19 April 2020).